

# Characterization of Subwavelength Plastic Fiber Utilizing Terahertz Time-Domain Spectroscopy

Borwen You<sup>a</sup>, Tze-An Liu<sup>b</sup>, Jin-Long Peng<sup>b</sup>, Ci-Ling Pan<sup>c</sup>, Ja-Yu Lu<sup>\*a</sup>

<sup>a</sup>Institute of Electro-Optical Science and Engineering, National Cheng Kung University, 1 University Road, Tainan 70101, Taiwan, R.O.C.

<sup>b</sup>Center for Measurement Standards, Industrial Technology Research Institute, 321, Sec.2, Kuang Fu Road, Hsinchu 30011, Taiwan, R.O.C.

<sup>c</sup>Department of Photonics and Institute of Electro-Optical Engineering, National Chiao Tung University, 1001 University Road, Hsinchu 30010, Taiwan, R.O.C.

## ABSTRACT

We present the first characterization of a simple subwavelength-diameter plastic wire by using wideband terahertz time-domain spectroscopy. The propagation characteristics including waveguide dispersion, group velocity, and attenuation constant of various plastic wires with different diameters and refractive indices are studied. The experimental results show the subwavelength plastic wire has extremely low waveguide dispersion and low attenuation constant ( $<0.01\text{cm}^{-1}$ ) at its THz transmission band due to much reduced fractional power delivered inside the lossy core, which is consistent with the theoretical calculations. With the large evanescent-fields, the subwavelength plastic wire has capability to integrate with micro-fluid channel for sensitive bio-sensing applications.

**Keywords:** THz, THz TDS, terahertz time domain spectroscopy, subwavelength fiber, subwavelength THz plastic fiber, plastic fiber, THz waveguide, THz fiber, waveguide dispersion, fiber dispersion, fiber attenuation

## 1. INTRODUCTION

Recently terahertz (THz) technology is tremendous developed and attracts lots of attention in imaging, sensing and spectroscopy. To make THz system more compact, it is necessary to develop THz fiber or waveguide to replace the bulky components. Various THz waveguides [1-4] including metal wires and dielectric fibers have been demonstrated and developed. However they have either high attenuation or poor coupling efficiency. For the communication, endoscope [5] and sensing applications, a low loss and low dispersion THz fiber is highly desired. In recent years it is significantly interested in dielectric optical nanowires[6] called as subwavelength fibers, whose core diameter is much smaller than guiding wavelength. One portion of power is confined around the fiber in air cladding, resulted from specific condition of fundamental mode. Subwavelength plastic fibers can be operated as extremely low loss fibers in THz frequency range due to most of THz power transmitted outside the lossy core [7, 8]. We apply terahertz time domain spectroscopy (THz-TDS), which provides the complex refractive index of materials within THz range, to study attenuation and dispersion of subwavelength THz plastic fibers. The attenuation and dispersion properties of subwavelength THz plastic fiber are investigated with different core diameter and material via THz-TDS. A theoretical model, based on electromagnetic wave theory in cylindrical dielectric, is applied to analyze the tendency of fiber dispersion while changing fiber core diameter or material. The consistency could be observed between theory and measured results. Based on the theory model, we try to use THz wave propagating outside the fiber, named as THz evanescent wave, to sense bio-medical specimen. This application is realized by sensing powders and liquids with different refractive indexes.

\* [jayu@mail.ncku.edu.tw](mailto:jayu@mail.ncku.edu.tw); +886-6-2757575 ext 65293; FAX:+886-6-2747955

## 2. THEORETICAL MODEL

### 2.1 Single Mode Condition of Subwavelength THz Plastic Fiber

Subwavelength THz plastic fiber is constructed of plastic circular core with infinite air cladding and a step-index profile. It transmits single mode,  $HE_{11}$ , based on equation (1). Fig. 1 shows the single mode condition of different fiber diameters, as a function of THz wavelength. The refractive index of fiber made by polystyrene (PS) is around 1.59 [9] in THz region. From the result it can be confirmed that 0.7~4.5mm-THz wave is propagated by single mode through the 300 $\mu$ m- and 400 $\mu$ m-diameter PS wires. Similarly it can be found that a 300 $\mu$ m-diameter -polyethylene (PE) wire, whose refractive index in THz region is around 1.50, can transmit single mode THz wave in the same wavelength range.

$$V \equiv \frac{2\pi}{\lambda} \cdot R \cdot \sqrt{n_{\text{cor}}^2 - n_{\text{cld}}^2} \leq 2.405 \quad (1)$$

where

$\lambda$  : wavelength

R : core radius

$n_{\text{cor}}$  : core refractive index

$n_{\text{cld}}$  : cladding refractive index

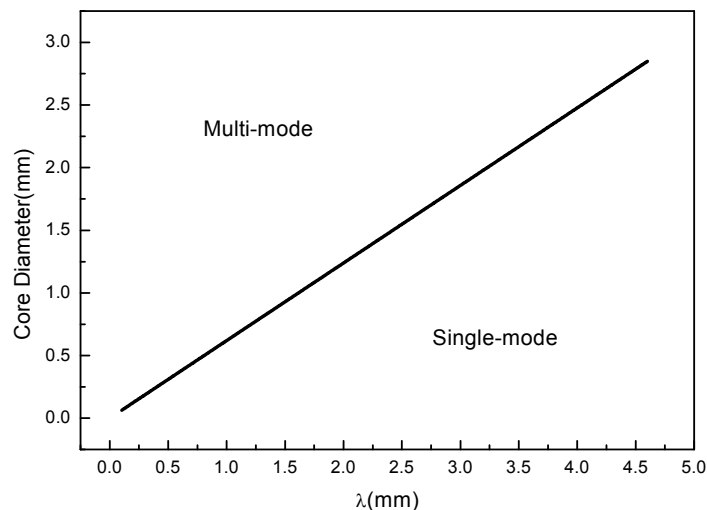


Fig.1 Single mode condition of an air-cladding PS wire.

### 2.2 Evanescent Wave of Subwavelength THz Plastic Fiber

The power distribution around subwavelength THz plastic fiber is concerned for the practical application in THz bio-medical sensing and THz communication. Fig.2 illustrates the fractional power inside and outside the core [6] of PS wire and the distributed result affects the fiber loss and dispersion in THz spectrum [7, 8]. For the larger diameter it confines more power inside the core and for the shorter THz wavelength it is easier to be confined in the core. On the other hand the z-axis power [6] in the cross section of plastic wire can be observed in Fig. 3, which compares the difference between 300 $\mu$ m-diameter PE and PS wires at different THz wavelengths. Obviously PS wire has a higher capability, compared with PE wire, to confine the THz wave surrounding the fiber core when the wavelength is increased longer than 1mm.

### 2.3 Fiber Dispersion of Subwavelength THz Plastic Fiber

Fiber dispersion, existing in any fiber or waveguide, can broaden the propagating pulse. It is not exclusive for subwavelength THz plastic fiber. Theoretically the fiber dispersion includes waveguide and material dispersion.

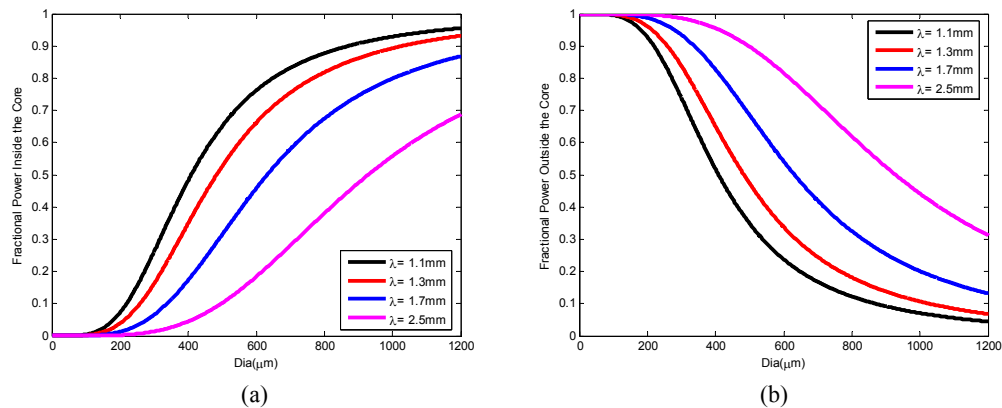


Fig.2 Power ratio for different diameters of PS wire at different THz wavelengths; a) fractional power inside the core; b) fractional power outside the core.

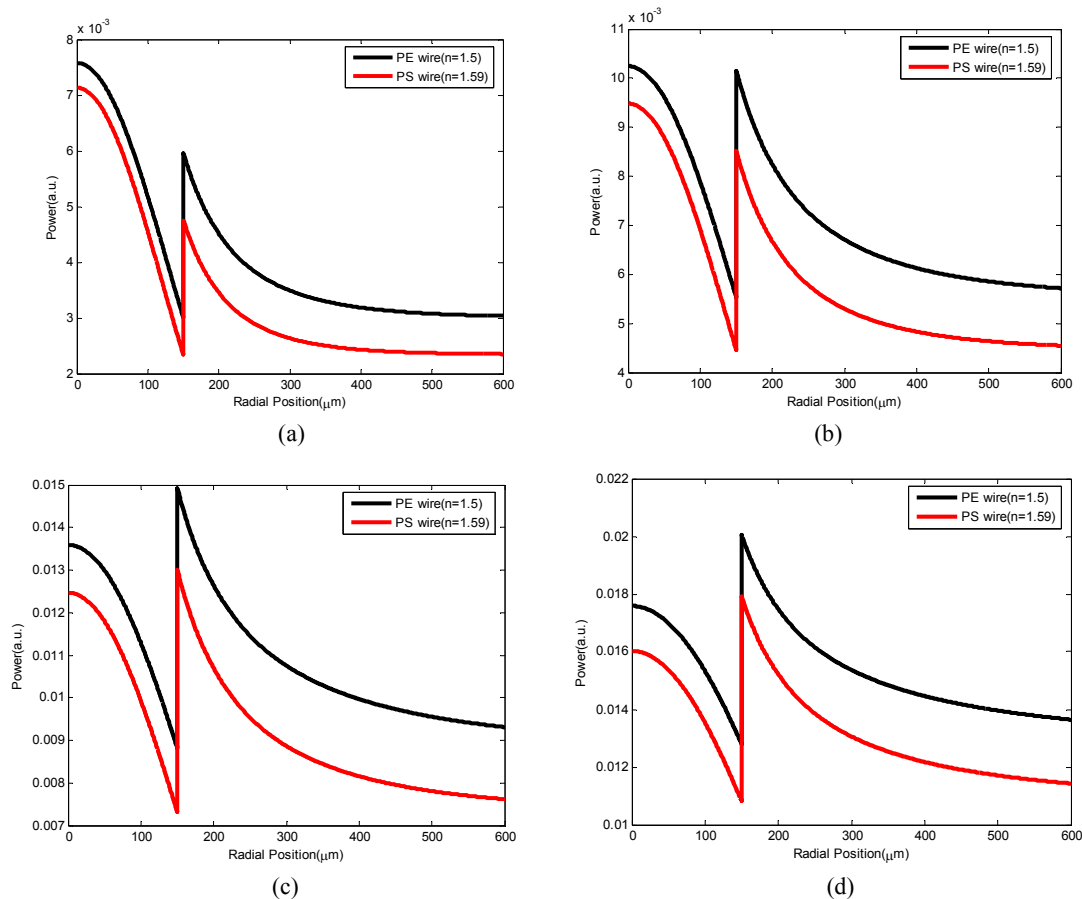


Fig. 3 Power distribution in cross section of 300μm-diameter PE and PS wires at different THz wavelengths; a) 0.8mm; b) 1.0mm; c) 1.2mm; d) 1.4mm.

However, for the refractive indexes of PE and PS plastic materials in THz spectrum are almost constant [9]; therefore, the material dispersion can be ignored in the discussion. Equation (2) shows the definition of waveguide dispersion and group velocity for subwavelength THz plastic fibers. The group velocity and waveguide dispersion for PS plastic wire is illustrated in Fig. 4 and Fig.5. For the longer THz wavelength and smaller diameter wire, the group velocity is

approached to light speed in the air and group velocity is decreased while increasing fiber diameter or decreasing THz wavelength. Besides the effect, the group velocity is converged to constant velocity,  $v_g=c/n_{cor}$ , when THz wavelength is decreased for larger wire core. Additionally it is found that the waveguide dispersion of plastic wire with a smaller diameter has more negative dispersion and the similar and it is approached to zero-dispersion for the increasing wavelength.

$$D_{WG} = \frac{d(V_g^{-1})}{d\lambda} \tag{2}$$

where

$V_g$  : Group velocity

$$V_g = \frac{c}{n_{cor}^2} \cdot \frac{\beta}{k} \cdot \frac{1}{1-2\Delta(1-\eta)}$$

$c$  : light speed in air

$\beta$  : propagation constant

$$k = \frac{2\pi}{\lambda}$$

$$\Delta \equiv \frac{1}{2} \cdot \left[ 1 - \left( \frac{n_{cld}}{n_{cor}} \right)^2 \right]$$

$\eta$  : Fractional power inside the core

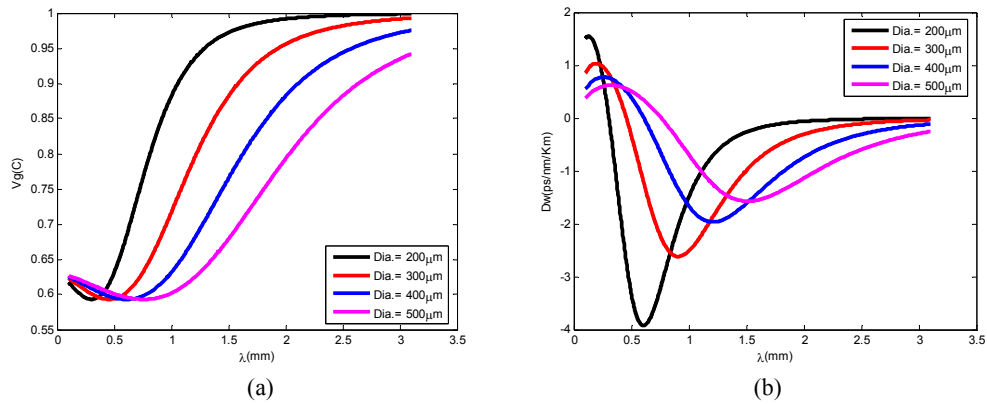


Fig. 4 a) Group velocity b) waveguide dispersion of subwavelength THz PS plastic fiber at different THz wavelengths.

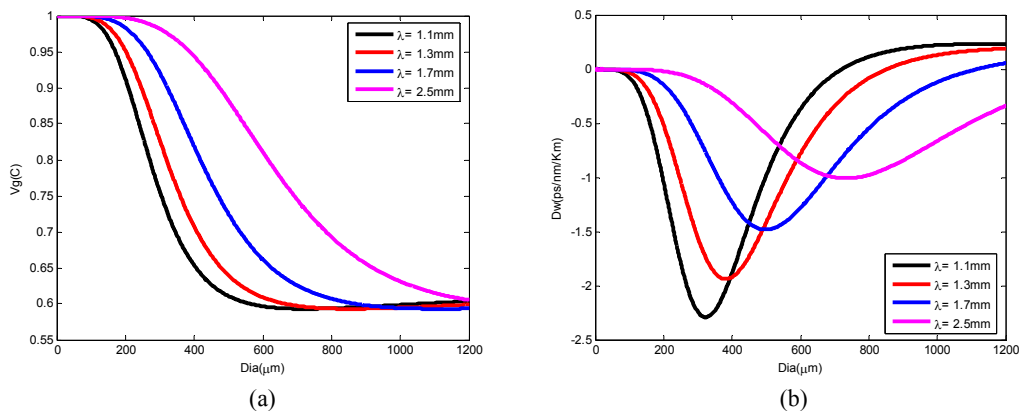


Fig. 5 a) Group velocity b) waveguide dispersion of subwavelength THz PS plastic fiber with different wire diameters.

### 3. CONFIGURATION AND MEASURED RESULTS

#### 3.1 Configuration of THz Time-Domain Spectroscopy

Terahertz time domain spectroscopy (THz-TDS) provides the method to analyze fiber dispersion and power attenuation. Fig. 6 shows the configuration of THz TDS system. A mode-locked Ti:sapphire laser with a center wavelength of 800nm, 100fs-pulse duration and 100MHz-repetition rate was used to excite THz emitter and detector. THz emitter and detector are LT-GaAs based photoconductive antennas with 5μm electrode gap. The generated THz wave is collimated and coupled to the fiber by means of off-axis parabolic mirrors.

#### 3.2 Power Attenuation

The propagation attenuation of THz wave through subwavelength THz plastic fiber is measured by cut-back method [7] and the coefficient is calculated from equation (3) in which the  $P_1$  and  $P_2$  are the THz powers passing through two different wire lengths. Fig. 7 shows the measured attenuation coefficient of PS and PE wires in THz spectrum. The loss in shorter wavelength spectrum, less than 0.85mm, is resulted from the material absorption [8]. In the reference [10] the PS bulk absorption is around  $0.27 \text{ cm}^{-1}$  for THz wave and that of PE bulk is around  $0.04 \text{ cm}^{-1}$ , which is lower than PS material. However, the minimum attenuation of PS wire is lower than that of PE wire due to the different fractional power distribution between 0.85~1.05mm-wavelength. In Fig. 3(a) and (b) it is found that PE wire has higher fractional power surrounding the fiber core and it will induce the major loss contributed by the variation of wire diameter [8]. This is the reason why PE wire has more loss in 0.85mm~1.05mm-wavelength. When the THz wavelength increases longer than 1.05mm, the fractional powers surrounding the wires are changed as Fig. (c) and (d). PS wire has more power surrounding the fiber core to generate more loss than that of PE wire.

$$\alpha = \frac{\ln\left(\frac{P_1}{P_2}\right)}{|L_1 - L_2|} \quad (3)$$

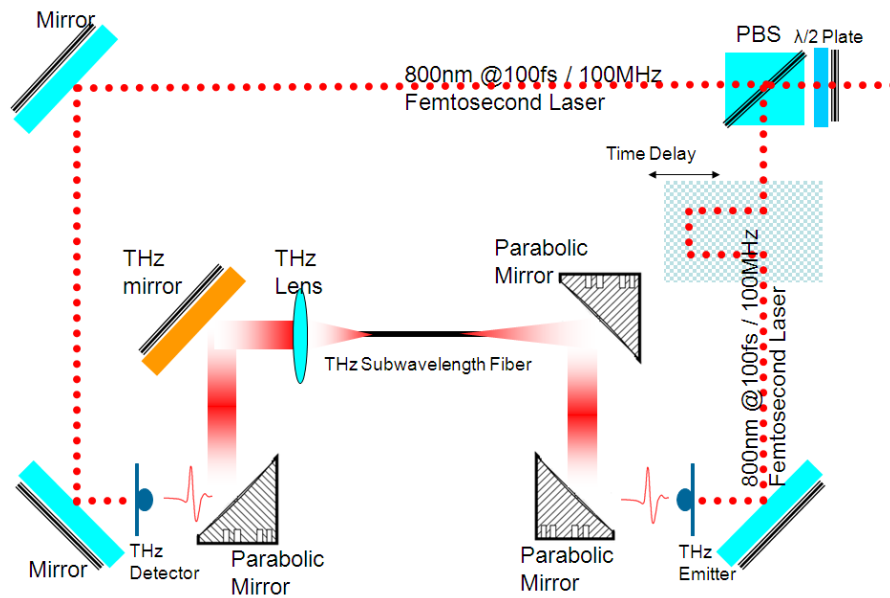


Fig. 6 THz-TDS configuration

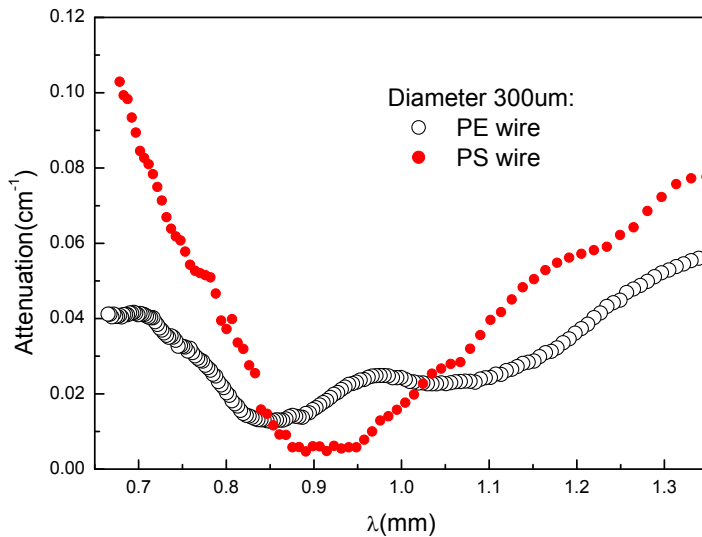


Fig. 7 Power attenuation of diameter-300µm PE and PS wires

### 3.3 Waveguide Dispersion

Besides the fiber attenuation, it was observed the broadened THz pulse propagating along PS wire is severer in longer wire length, which is shown in Fig. 8. Waveguide dispersion dominates the pulse broadening effect as the express of theoretical model. Waveguide dispersion is analyzed from the phase difference of THz pulses transmitted along two different wire lengths. The theory and measured THz waveguide dispersion,  $D_{WG}$ , of 300µm- and 400µm-diameter PS wires are shown in Fig. 9(a). The tendency of theory and measured results are consistent. The smaller diameter of subwavelength fiber has more evident negative dispersion and its deep will be shifted to shorter wavelength range, which is similar to the result of optical nanowire [6]. The waveguide dispersion of diameter-300µm PE and PS wires is measured and compared with the theory, illustrated in Fig. 9(b). PS wire has obvious negative waveguide dispersion and the deep is shifted to longer wavelength range due to its higher refractive index compared with PE wire. Based on the results we could transmit desired THz wave to zero-dispersion by means of wire index or diameter.

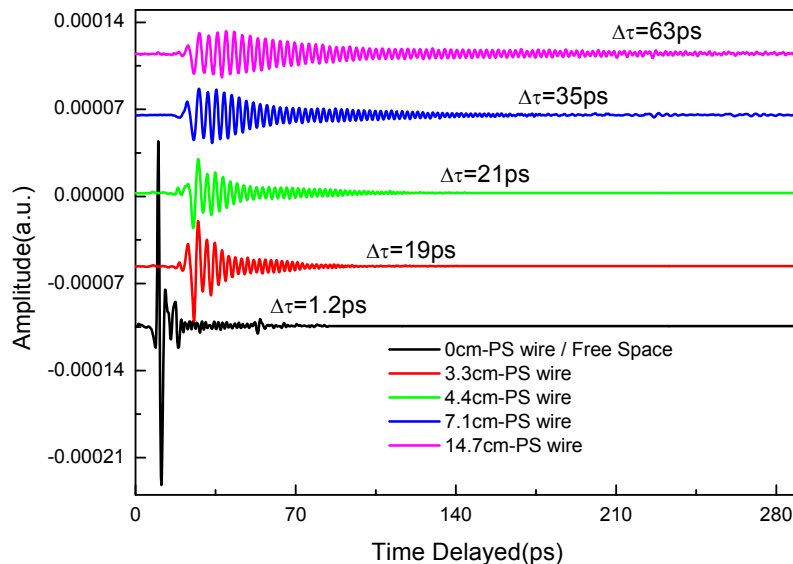


Fig. 8 THz pulse waveform transmits along different lengths of PS wire

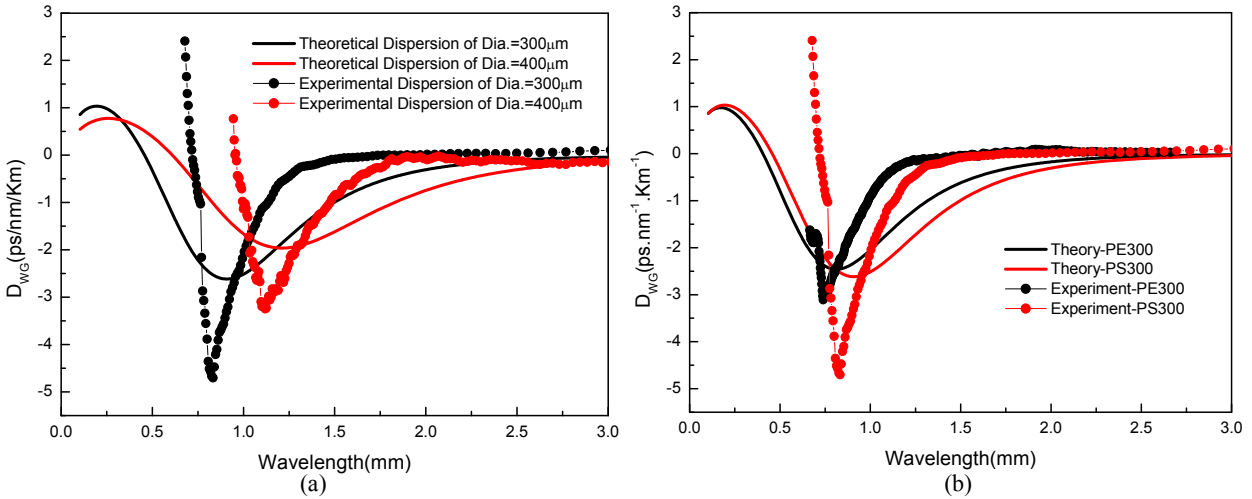


Fig. 9 a) Waveguide dispersion of 300µm- and 400µm- diameter PS wires; b) waveguide dispersion of 300µm- diameter PE and PS wires

## 4. APPLICATION OF BIO-MEDICAL SENSING

### 4.1 Concept

We can use the evanescent THz wave of subwavelength THz plastic fiber to sense the specimens outside the fiber. The mechanism is resulted from the phase shift when the cladding index is changed for THz wave interacting with samples. Theoretically the negative waveguide dispersion is decreased due to slight variation of cladding index, illustrated in Fig. 10. One poly propylene (PP) holder, whose refractive index in THz is around 1.50 [10], is put under the PS wire and the specimen is filled in the sensitive area. Fig. 11 illustrates the simple drawing of the setup and the PE film put on the sensitive area is optional for liquid sensing to prevent from evaporating. The effective cladding index is considered as equation (4) including different ratio of air and sample portion depending on the wire position above the sample.

$$n_{eff} = \sigma \cdot n_{AIR} + (1 - \sigma) \cdot n_{sample} \quad (4)$$

where

$\sigma$  : air ratio in THz wave

$n_{AIR}$  : index of air (= 1)

$n_{sample}$  : Sample index in THz

### 4.2 Sensing Results

From this concept we test different powders and liquids to observe the dispersion variation of 300µm-diameter PS wire. For example, Tryptophan [11] and PE powders [10], whose refractive indexes in THz are 1.17 and 1.5 individually, are used in powder sensing and Fig. 12 illustrates the theory and measured waveguide dispersions. It shows the negative peak dispersion is decreased while the interaction of THz wave in PE powder instead of tryptophan. In theory it is resulted from the higher refractive index of PE powder compared with tryptophan. When we consider 60%-air ratio in the cross section of the PS wire, the effective cladding indexes for PE and tryptophan powders are 1.068 and 1.2 individually. The varied percentage of negative peak dispersion for theory and measured result are consistently around 17%. In the same way this concept can be used in liquid sensing for water [12] and alcohol [13], whose refractive indexes in THz are 2.6 and 1.45 individually. When we consider the 75%-air ratio in cladding, the effective cladding indexes are 1.11 and 1.4 for alcohol and water individually. Fig. 13 shows the same variation of negative peak dispersion for water and alcohol are around 40%.

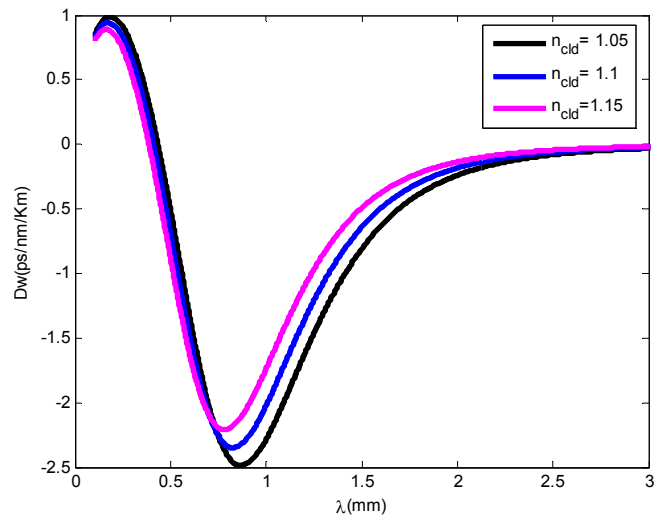


Fig.10 The waveguide dispersion of diameter-300 $\mu$ m PS wire for different cladding indexes

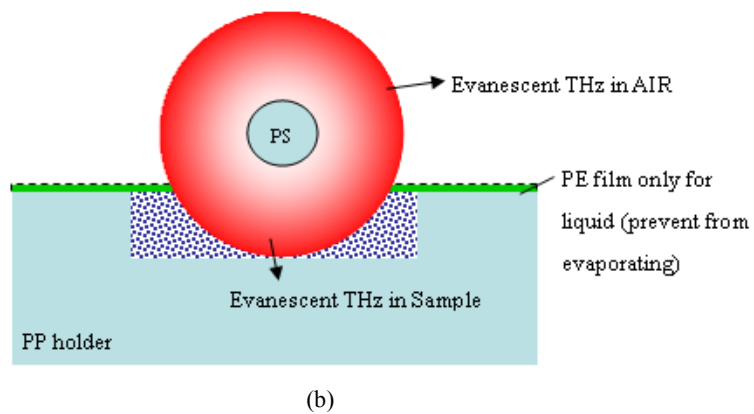
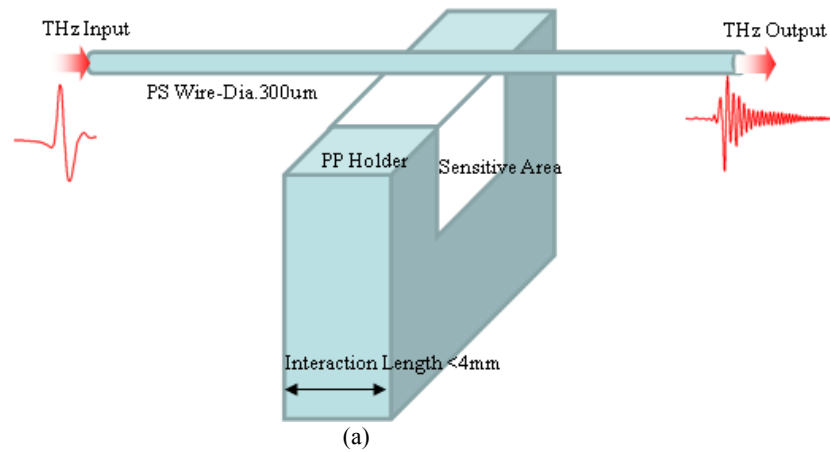


Fig. 11 Sensing configuration for a) 3D version; b) end-face version



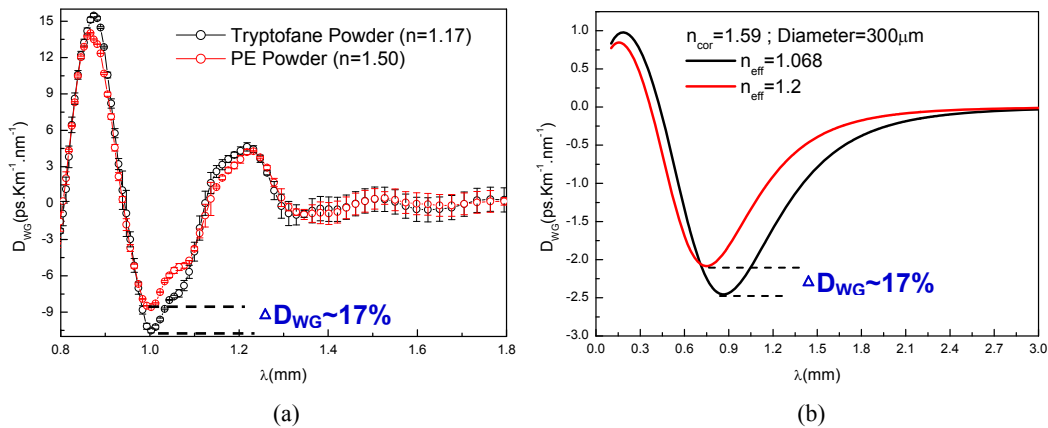


Fig. 12 The same variation percentage of negative peak dispersion between PE and tryptophan powders. a) Measured result; b) theory for effective cladding index considering 60%-air-ratio.

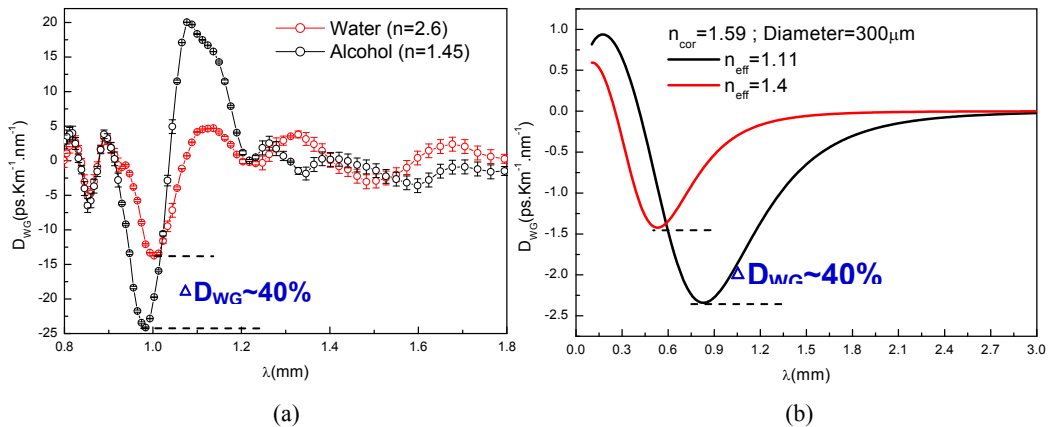


Fig. 13 The same variation percentage of negative peak dispersion between water and alcohol liquids. a) Measured result; b) theory effective cladding index considering 75%-air-ratio.

## 5. CONCLUSION

The attenuation and dispersion properties of subwavelength THz plastic fiber have been investigated utilizing THz time domain spectroscopy. It is demonstrated that the minimum attenuation of subwavelength THz plastic fiber is independent from material absorption. We analyze the power fraction surrounding fiber core for PS and PE wires to express the THz spectrum loss. For the waveguide dispersion, the tendency resulted from changing core diameter and mater is reasonable. Therefore, the zero dispersion and low loss fiber can be achieved by specific diameter and material of plastic wire for any THz wave. Besides studying the properties of subwavelength THz plastic fibers we also demonstrate the evanescent field of subwavelength THz plastic fiber can be used to sense powders and liquids.

## REFERENCES

- [1] Frankel, M.Y., Gupta, S., Valdmanis, J.A., Mourou, G.A., "Terahertz attenuation and dispersion characteristics of coplanar transmission lines", IEEE Transactions on microwave theory and techniques, **39** (6), 910 – 916(1991).
- [2] R. Mendis and D. Grischkowsky, "Plastic ribbon THz waveguides", J. Appl. Phys. **88**(7), 4449 (2000).
- [3] S. P. Jamison, R. W. McGowan, and D. Grischkowsky, "Single-mode waveguide propagation and reshaping of sub-terahertz pulses in sapphire fibers", J. Appl. Phys. **76**, 15, 1987-1989 (2000).
- [4] McGowan, R W; Gallot, G; Grischkowsky, D, "Propagation of ultrawideband short pulses of terahertz radiation through submillimeter-diameter circular waveguides", Optics Letters, **24** (20), 1431-1433 (1999).

- [5] J.-Y. Lu, C.-M. Chiu, C.-C. Kuo, C.-H. Lai, H.-C. Chang, Y.-J. Hwang, C.-L. Pan, and C.-K. Sun, "Terahertz scanning imaging with a subwavelength plastic fiber", *Appl. Phys. Lett.*, **92**, 084102 (2008).
- [6] Limin Tong, Jingyi Lou, Eric Mazur, "Single-mode guiding properties of subwavelength-diameter silica and silicon wire waveguides", *Optics Express*, **12**, (6), 1025(2004).
- [7] Li-Jin Chen, Hung-Wen Chen, Tzeng-Fu Kao, Ja-Yu Lu, and Chi-Kuang Sun, "Low-loss subwavelength plastic fiber for terahertz waveguiding", *Optics Letters*, **31**(3), 308(2006).
- [8] Hung-Wen Chen, Yu-Tai Li and Ci-Ling Pan, Jeng-Liang Kuo, Ja-Yu Lu, Li-Jin Chen, and Chi-Kuang Sun, "Investigation on spectral loss characteristics of subwavelength terahertz fibers", *Optics Letters*, **32** (9), 1017(2007).
- [9] R. Piesiewicz, C. Jansen, S. Wietzke, D. Mittleman, M. Koch & T. Kürner, "Properties of Building and Plastic Materials in the THz Range", *Int J Infrared Milli Waves*, DOI 10.1007/s10762-007-9217-9.
- [10] James W. Lamb, "Miscellaneous data on materials for millimetre and submillimetre optics", *International Journal of Infrared and Millimeter Waves*, **17**(12), 1997(1996).
- [11] B. Yu, F. Zeng, Y. Yang, Q. Xing, A. Chechin, X. Xin, I. Zeylikovich and R. R. Alfano, "Torsional Vibrational Modes of Tryptophan Studied by Terahertz Time-Domain Spectroscopy", *Biophysical Journal*, **86**, 1649–1654(2004).
- [12] L. Thrane, R.H. Jacobsen, P. Uhd Jepsen, S.R. Keiding, "THz reflection spectroscopy of liquid water", *Chemical Physics Letters*, **240**, 330(1995).
- [13] Hideaki Kitahara, Takuma Yagi, Keisuke Mano and Mitsuo Wada Takeda, "Dielectric Characteristics of Water Solutions of Ethanol in the Terahertz Region", *Journal of the Korean Physical Society*, **46**(1), 82(2005).